

Collective modes across the soliton-droplet crossover in binary Bose mixtures

Alberto Cappellaro,^{1,*} Tommaso Macrì,^{2,†} and Luca Salasnich^{1,3,‡}

¹*Dipartimento di Fisica e Astronomia "Galileo Galilei", Università di Padova, via Marzolo 8, 35131 Padova, Italy*

²*Departamento de Física Teórica e Experimental, Universidade Federal do Rio Grande do Norte, and International Institute of Physics, Natal-RN, Brazil*

³*CNR-INO, via Nello Carrara, 1 - 50019 Sesto Fiorentino, Italy*

(Dated: May 16, 2018)

We study the collective modes of a binary Bose mixture across the soliton to droplet crossover in a quasi one dimensional waveguide with a beyond-mean-field equation of state and a variational Gaussian ansatz for the scalar bosonic field of the corresponding effective action. We observe a sharp difference in the collective modes in the two regimes. Within the soliton regime modes vary smoothly upon the variation of particle number or interaction strength. On the droplet side collective modes are inhibited by the emission of particles. This mechanism turns out to be dominant for a wide range of particle numbers and interactions. In a small window of particle number range and for intermediate interactions we find that monopole frequency is likely to be observed. In the last part we focus on the spin-dipole modes for the case of equal intraspecies interactions and equal equilibrium particle numbers in the presence of a weak longitudinal confinement. We found that such modes might be unobservable in the real-time dynamics close to the equilibrium as their frequency is higher than the particle emission spectrum by at least one order of magnitude in the droplet phase. Our results are relevant for experiments with two-component BECs for which we provide realistic parameters.

I. INTRODUCTION

The exquisite control of parameters in ultracold quantum gases, culminated with the achievement of Bose-Einstein condensation in alkali vapors, boosted a great experimental effort to engineer multi-component systems [1–3]. From the theoretical standpoint, the spinorial nature of the order parameter and its complex dynamics, as in ^3He - ^4He mixtures and three-fluids models [4–6], enable an ample variety of interesting physical effects. They span from persistent supercurrent and internal Josephson effect [7–9], itinerant ferromagnetism in fermionic mixtures [10, 11], to more exotic topics as the research for analogues of Hawking radiation in bosonic mixtures [12–14] and spin-orbit physics [15–18].

More recently, the theoretical proposal of the existence of self-bound quantum droplets in binary bosonic mixtures by Petrov [19, 20] opened new opportunities for the investigation of non trivial quantum phases in BECs. Dilute quantum droplets were first observed in a single component dipolar condensates of dysprosium [21–23] even in absence of external confinement [24], confirming droplet self stability. Experiments with binary mixtures were recently performed using two internal states of ^{39}K in Barcelona [25, 26] and Florence [27] both in three dimensions and in quasi-one dimensional setups. Theoretical work on both dipolar [28–32] and binary BECs [33–35] well describes such experiments in a variety of regimes by the inclusion of leading Gaussian corrections to the

mean field equation of state.

In a recent experiment [26], the formation of dilute self-bound states in a two-component BEC was studied in a tight optical waveguide. Interestingly, above a critical value of the magnetic field a smooth crossover interpolating between droplets and bright soliton states was observed. Below such critical magnetic field and for small particle numbers a bistable region is detected, corresponding to different minima of the energy functional. Importantly, droplets appear naturally as a competition of meanfield and quantum fluctuation energies with opposite sign. Solitons, on the other hand, are excitations appearing genuinely in low dimensional systems. If the 1D interaction strength is repulsive (self-defocusing nonlinearity) one recovers localized dark solitons, while for attractive condensates (self-focusing nonlinearity) one finds bright solitons. Both dark and bright solitons have been observed experimentally with atomic BECs [36].

In this work we study the collective modes of a two-component Bose gas in an optical waveguide along the crossover from solitons to droplets. Collective modes are an essential tool to identify and characterize the behavior of a quantum system both at zero and at finite temperature. For single component BEC with contact interactions in a confining potentials they have been studied throughly both theoretically and experimentally [37]. In the presence of non-local interactions, such as soft-core [38–41] or dipolar potentials [42, 43], or internal coupling in multi-component systems [33, 34], collective modes turn out to be crucial to detect quantum phase transitions from the uniform state to a structured ground state configuration. Binary systems naturally support modes where the two component move in phase, such as monopole and quadrupole oscillations, which are ex-

* cappellaro@pd.infn.it

† macri@fisica.ufrr.br

‡ luca.salasnich@unipd.it

pected to be the lowest energy excitations. In these simple cases the two components share the same spatial wavefunction over the oscillation period. More interestingly, there exists cases in which the spinorial nature of the order parameter allows nontrivial collective modes where the internal components move out of phase around the equilibrium configuration. The simplest case is represented by the so-called spin-dipole excitation. For a repulsive two-component Bose gas the spin-dipole oscillation frequency depends crucially on the presence of an external confining potential as well as on the reciprocal interaction strength and they were recently characterized in an experiment of the Trento group [44]. Remarkably, for attractive binary mixtures, spin-dipole oscillations may take place even in the absence of an external potential, the restoring force being proportional to the interspecies interaction. In this paper we characterize such modes highlighting the combined effect of the standard mean-field attraction and the beyond-mean field corrections to the oscillation frequency. We employ a variational approach based on a Gaussian ansatz for the space modes of the two components, which has been proven to perform well close to the equilibrium configuration. We find striking differences of the collective modes between droplets and solitons. Namely, in the soliton phase we are able to generalize well known results of quasi-1D BECs. In the droplet regime we find that collective modes are generically inhibited as they have energies higher than the particle emission spectrum for a wide range of available experimental parameters.

In Section II we summarize the formalism and the variational results of the ground state of the two-component mixtures with equal masses. In Section III we derive the collective modes in the crossover from soliton to droplet for a wide range of particle numbers and interaction strength for the experimentally relevant case of ^{39}K within the variational approach. Then, in Section IV, we focus on the spin-dipole oscillation mode, which is characteristic of a two-component mixture. We specialize to the case of equal intra-species interaction strength for different particle numbers and compare it with the particle emission spectrum. Finally, in Section V, we highlight the connection of the present study with current experiments on mixtures and give some perspectives for future work in the Conclusions.

II. SOLITON-TO-DROPLET CROSSOVER

We begin by considering a Bose gas made of atoms in two different hyperfine states in a volume L^3 . Each component can be described by a complex field ψ_i ($i = 1, 2$), whose dynamics results from the following real-time low-energy effective action

$$S = \int dt d^3\mathbf{r} \left[\sum_{j=1,2} \frac{i\hbar}{2} (\psi_j^* \partial_t \psi_j - \psi_j \partial_t \psi_j^*) - \mathcal{E}_{\text{tot}}(\psi_1, \psi_2) \right]. \quad (1)$$

The total energy density \mathcal{E}_{tot} reads

$$\begin{aligned} \mathcal{E}_{\text{tot}} = & \sum_{j=1,2} \left[\frac{\hbar^2}{2m} |\nabla \psi_j|^2 + V_{\text{ext}}(\mathbf{r}) |\psi_j|^2 + \frac{1}{2} g_{jj} |\psi_j|^4 \right] \\ & + g_{12} |\psi_1|^2 |\psi_2|^2 + \mathcal{E}_{\text{BMF}}(\psi_1, \psi_2), \end{aligned} \quad (2)$$

where $V_{\text{ext}}(\mathbf{r})$ is an external confining potential and $g_{jk} = 4\pi\hbar^2 a_{jk}/m$, a_{jk} being the intra- (with $a_{jk} \propto \delta_{j,k}$) and inter-species ($j \neq k$) scattering lengths, $n_j = |\psi_j|^2$ is the density of the species j . The beyond-mean-field term \mathcal{E}_{BMF} arises from the zero-point energy of Bogoliubov collective excitations [19, 45], namely

$$\mathcal{E}_{\text{BMF}} = \frac{8}{15\pi^2} \left(\frac{m}{\hbar^2} \right)^{3/2} (g_{11} n_1)^{5/2} f \left(\frac{g_{12}^2}{g_{11} g_{22}}, \frac{g_{22} n_2}{g_{11} n_1} \right) \quad (3)$$

with $f(x, y) = \sum_{\pm} [1 + y \pm \sqrt{(1-y)^2 + 4xy}]^{5/2} / (4\sqrt{2})$. In this first section, the calculation leading to the ground state properties can be simplified by assuming the two components occupying the same spatial mode [19, 20]. The bosonic fields can then be redefined as $\psi_j = \sqrt{n_j} \phi(\mathbf{r}, t)$. This assumption neglects the inter-component dynamics, resulting inadequate to probe, for example, spin-dipole oscillations. In Sec. IV, within the variational framework, we present a modified Gaussian ansatz to include this feature in our study. The minima of mean-field energy density Eq. (3) fixes the ratio between the components of the population at which the spatial overlap is maximized, i.e. $N_1/N_2 = \sqrt{a_{22}/a_{11}}$ [19, 25], which we assume throughout this section. By defining $\Delta a = a_{12} + \sqrt{a_{11}a_{22}}$, Eq. (2) can be expressed as

$$\begin{aligned} \mathcal{E}_{\text{tot}} = & \frac{\hbar^2 n_{\text{tot}}}{2m} |\nabla \phi|^2 + n_{\text{tot}} V_{\text{ext}}(\mathbf{r}) |\phi|^2 \\ & + \frac{4\pi\hbar^2}{m} \frac{\Delta a \sqrt{a_{22}/a_{11}}}{\left(1 + \sqrt{a_{22}/a_{11}} \right)^2} n_{\text{tot}} |\phi|^4 \\ & + \frac{256\sqrt{\pi}\hbar^2}{15m} \left(\frac{n_{\text{tot}} \sqrt{a_{11}a_{22}}}{1 + \sqrt{a_{22}/a_{11}}} \right)^{5/2} f \left(\frac{a_{12}^2}{a_{11}a_{22}}, \sqrt{\frac{a_{22}}{a_{11}}} \right) |\phi|^5, \end{aligned} \quad (4)$$

where $n_{\text{tot}} = n_1 + n_2$. Inspired by the experiment described in [26], from now on, we consider a quasi-one dimensional optical waveguide. Then we take a harmonic confinement on a transverse plane, so $V_{\text{ext}} = \frac{1}{2} m \omega_{\perp}^2 (x^2 + y^2)$. The presence of a harmonic potential defines a characteristic length scale, namely $a_{\perp} = \sqrt{\hbar/(m\omega_{\perp})}$. In the following, all lengths are in units of a_{\perp} and energies in units of $\hbar\omega_{\perp}$. Scattering length will be rescaled in units of the Bohr radius a_0 for convenience. The beyond-mean-field diagram and the static properties of the ground-state configurations have been studied in [26].

The properties of the system can be analytically explored by taking a Gaussian ansatz

$$\phi(\mathbf{r}) = \sqrt{\frac{L^3}{\pi^{3/2} \sigma_r^2 \sigma_z}} \exp \left(- \sum_{r_i=x,y,z} \frac{r_i^2}{2\sigma_{r_i}^2} \right) \quad (5)$$

whose variational parameters are σ_r and σ_z . The choice of normalization factor ensures that the original condition $||\psi||^2 = N$ is preserved. By replacing Eq. (5) in Eq. (4) and taking the infinite volume limit, the variational energy per particle is given by [26]

$$\begin{aligned} \frac{E}{N\hbar\omega_{\perp}} &= \frac{1}{4} \left(\frac{1}{\tilde{\sigma}_x^2} + \frac{1}{\tilde{\sigma}_y^2} + \frac{1}{\tilde{\sigma}_z^2} \right) + \frac{\tilde{\sigma}_x^2 + \tilde{\sigma}_y^2}{4} \\ &+ \frac{2N\Delta\tilde{a}}{\sqrt{2\pi}\tilde{\sigma}_x\tilde{\sigma}_y\tilde{\sigma}_z} \frac{\sqrt{\tilde{a}_{22}/\tilde{a}_{11}}}{\left(1 + \sqrt{\tilde{a}_{22}/\tilde{a}_{11}}\right)^2} \\ &+ \frac{512\sqrt{2}}{75\sqrt{5}\pi^{7/4}} \frac{N^{3/2}}{(\tilde{\sigma}_x\tilde{\sigma}_y\tilde{\sigma}_z)^{3/2}} \left(\frac{\sqrt{\tilde{a}_{11}\tilde{a}_{22}}}{1 + \sqrt{\tilde{a}_{22}/\tilde{a}_{11}}} \right)^{5/2} \times \\ &\times f\left(\frac{\tilde{a}_{12}^2}{\tilde{a}_{11}\tilde{a}_{22}}, \sqrt{\frac{\tilde{a}_{22}}{\tilde{a}_{11}}}\right). \end{aligned} \quad (6)$$

The tilde signals that we are expressing a length in units of a_{\perp} . By means of Feshbach resonance [46], below a critical value of the magnetic field, the condition $\Delta a < 0$ is achieved. Here, due to the simultaneous presence of quantum fluctuations and external confinement, two different self-bound states can be observed. First, for low particles number or, equivalently small values of $|\Delta a|$, the ground state of the system corresponds to the so-called solitonic state, whose shape basically depends on the external trapping. Indeed, $\sigma_x = \sigma_y \sim a_{\perp}$, while the longitudinal one σ_z is much greater. It is important to remark the fact that beyond-mean-field corrections are not necessary for the stability of this state. Indeed quantities such as the energy and density profile are in good agreement with the mean-field solutions for bright solitons in BEC [48].

The situation changes by increasing the particle number or lowering Δa . Here, the system moves to an isotropic ground state ($\sigma_x = \sigma_y = \sigma_z < a_{\perp}$), effectively independent of the confinement aspect ratios. The existence of this self-bound state is enabled by taking into account the contribution of Gaussian quantum fluctuations in the variational energy of Eq. (3). These results are summarized in Fig. 1 where we plot the width as a function of N at fixed values of Δa (left panels) and, in turn, as a function of Δa for chosen values of N (right panels) computed via the Gaussian ansatz Eq. (5).

At fixed Δa , the system approaches the droplet state by increasing the particle number. In order to reach a pure isotropic state, the effective mean-field attraction, i.e. Δa , has to be strong enough. For example, at $\Delta a = -5.1 a_0$, σ_z remains two times larger than the radial width even at $N = 10000$, while for $\Delta a = -10.6 a_0$ the system approaches a spherical configuration already at approximately 5000 particles. For weak attractive interactions (small negative Δa) the shift from one bound state to the other occurs via a smooth crossover see e.g. Fig. 1 for $\Delta a = -8.7 a_0$. At stronger interactions (large negative Δa) the system undergoes a bistability where competing minima are present in the energy functional,

and lead to a sharp structural change of the condensate as in Fig. 1 at $\Delta a = -10.6 a_0$ [26]. A similar picture emerges by considering a fixed particles numbers and tuning the effective mean-field attraction as in the right panels of Fig. 1.

III. COLLECTIVE MODES IN THE VARIATIONAL APPROACH

A deeper insight into the differences between solitonic and droplet states can be reached by examining collective excitations frequencies around the minima of the variational energy of Eq. (6), given the Gaussian ansatz in Eq. (5). The variational Gaussian approach results to be particularly reliable in predicting collective excitations frequencies for a wide range of superfluid systems. As an example, in [34] a detailed analysis has been carried out by comparing the variational approach with numerical solutions of the Gross-Pitaevskii in purely 1D binary Bose mixtures. Concerning excitation frequencies, numerical and analytical predictions are shown to be in great agreement. Moreover, our theoretical framework was also applied to study droplet-configurations and surface effects in confined fermionic superfluids as in [47], where variational results are well reproduced by density-functional-theory simulations. By solving the eigenvalue problem of the Hessian matrix $\text{Hess}(E) = \frac{\partial^2 E}{\partial \sigma_i \partial \sigma_j}$ computed in the solitonic (or droplet) minimum, three different oscillation modes are allowed. In Fig. 2 we represent the three oscillation frequencies (ω_I , ω_{II} , ω_{III}) as predicted by the Gaussian ansatz.

In the solitonic state one frequency, labelled ω_I , can be easily excited, reflecting the absence of confinement along a direction. The other two modes are degenerate and converge to 2 (in units of $\hbar\omega_{\perp}$) as in a weakly interacting BEC [48]. The degeneracy of ω_{II} and ω_{III} is an obvious consequence of the cylindrical symmetry of the radial confinement. This structure is clear in the panel (d) of Fig. 2, where mode frequencies are depicted for the $N = 2000$ case: $\omega_{II} = \omega_{III} \simeq 2$, two order of magnitude higher than ω_I . The same feature survives by increasing the particles number (middle and bottom panel of Fig. 2) in the solitonic side of the crossover for low values of Δa .

In the droplet side of the crossover, Fig. 2 also shows the particle-emission-threshold $-\mu$. The chemical potential μ is obtained by differentiating the total energy in Eq. (4) with respect to N within the Gaussian ansatz in Eq. (5). In the solitonic state, $\mu > 0$ for every value of Δa and lies above ω_I and consequently this frequency can be excited and experimentally revealed. The eigenvector corresponding to ω_I displays the monopole character of this excitation, since $\mathbf{v}_I = \pm\alpha(1, 1, 1)^T$. Moving to the droplet-side of the crossover, frequencies lie above the emission threshold in agreement with the prediction of [19, 27]. This implies that excitations of the system are damped by expelling particles from the droplet in a

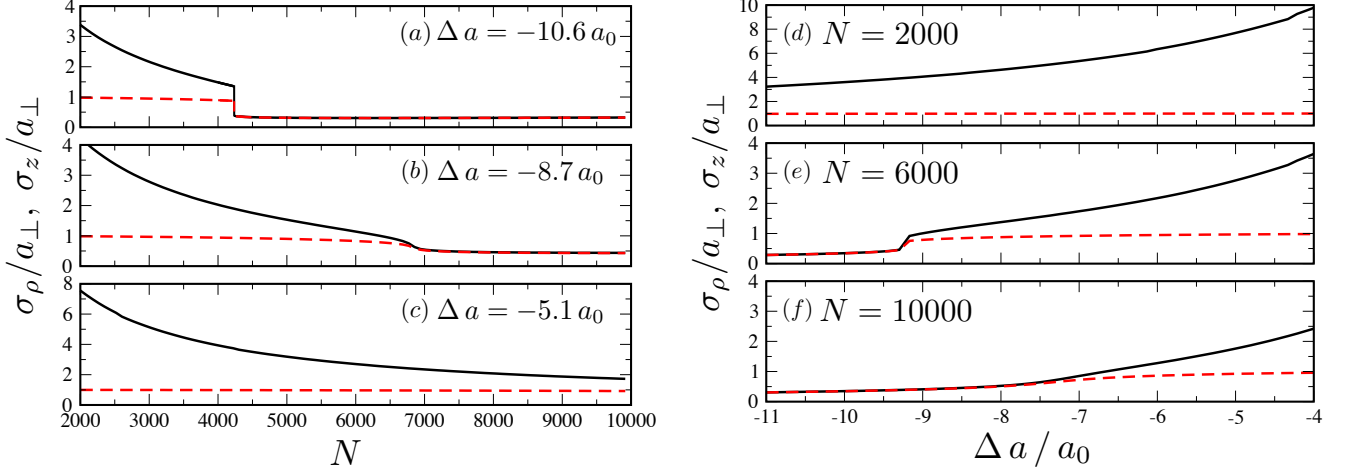


FIG. 1. Widths of the ground-state energy predicted by the variational Gaussian energy in Eq. (6). Widths σ_i with $i = x, y, z$ are expressed in units of the oscillator length $a_\perp = \sqrt{\hbar/(m\omega_\perp)}$ for several values of $\Delta a(a_0)$ (units of the Bohr's radius). In the plots σ_z (solid black line), the gaussian width along the longitudinal direction, and σ_ρ (red dashed line) along the transverse plane. Due to cylindrical symmetry of the confinement, $\sigma_x = \sigma_y$. Left panels: Variational widths as a function of the particles number N for three different values of (a) $\Delta a = -10.6$, (b) -8.7 , (c) -5.1 . In (a) a sharp change of σ_r and σ_z is observed for $N \approx 4200$ signaling a bistability. Right Panels: Variational widths as a function of Δa for three different values of (d) $N = 2000$, (e) 6000, (f) 10000.

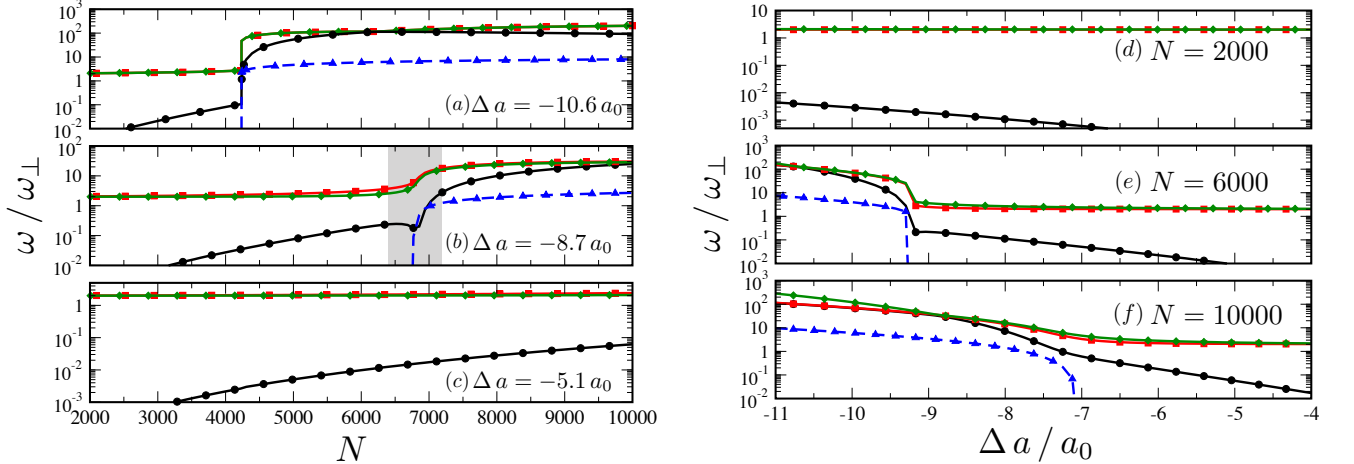


FIG. 2. Excitation frequencies ω_I , ω_{II} , ω_{III} and the particle-emission threshold $-\mu$, in units of $\hbar\omega_\perp$ as functions of Δa in units of Bohr's radius a_0 . The emission threshold (blue triangles) is shown only in the droplet side of the crossover. The excitation frequencies correspond to the eigenvalues of the Hessian matrix of Eq. (6) Left Panels: Frequencies as functions of the particle number N for three different values of the parameter (a) $\Delta a = -10.6$, (b) -8.7 , (c) -5.1 . In (b) the grey region denotes the interval of particle numbers where the monopole mode is lower than the particle emission spectrum in the droplet phase. See also Fig.3 for a magnification of this area. Right Panels: Frequencies as functions of Δa for three different values of $N = 2000$, (e) 6000, (f) 10000.

peculiar self-evaporation process. We also verified that, for $\Delta a = -5.1 a_0$, as in Fig. 2c, upon increasing the particle number to larger values one enters into the self-evaporation regime ($5.2 \cdot 10^4 < N < 1.4 \cdot 10^5$). Increasing even more the system size, self-evaporation ceases and the excitations are, at least in principle, observable. It is also interesting to observe that droplet length increases almost linearly with the particle number already

for $N \geq 4 \cdot 10^4$.

IV. SPIN-DIPOLE OSCILLATIONS

In this section we consider the relative dynamics between the two components of the mixture. We describe the oscillatory motion occurring when the two compo-

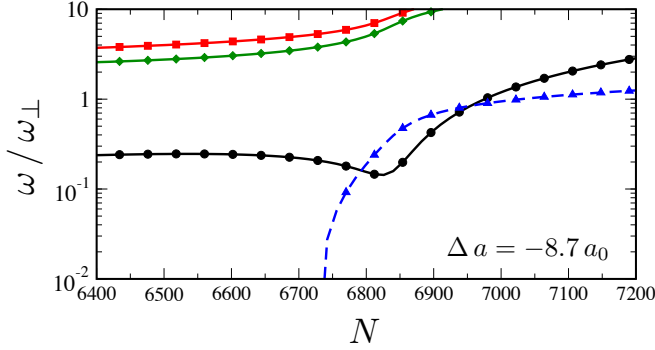


FIG. 3. *Excitation spectrum at the crossover soliton-droplet at $\Delta a = -8.7 a_0$.* Magnification of the grey region of Fig. 2(b) with $N = 6400 - 7200$. In the range $6780 \lesssim N \lesssim 6950$ monopole oscillations (black line-dots) are higher than the particle emission spectrum (dashed blue line - triangles).

ment are displaced from the center of the harmonic trap. To model their collective dynamics, we go beyond the assumption where the two components occupy the same spatial mode. We may introduce a weak confinement also along the z -axis with corresponding aspect ratio $\lambda_z = \omega_z / \omega_{\perp}$.

Then, we define a center of mass coordinate of each of the two components. The resulting Gaussian variational ansatz now reads

$$\psi_j = \sqrt{\frac{N_j}{\pi^{3/2} \sigma_r^2 \sigma_z}} e^{-\frac{x^2+y^2}{2\sigma_r^2}} \exp\left[-\frac{(z-z_j)^2}{2\sigma_z^2} + i\alpha_j z\right], \quad (7)$$

where the fields ψ_1 and ψ_2 obey the normalization condition $\int d^3\mathbf{r} |\psi_j|^2 = N_j$. In the equation above we assumed cylindrical symmetry $\sigma_x = \sigma_y = \sigma_r$. $\{\alpha_i\}_{i=1,2}$ describe the corresponding slopes of $\{z_i\}_{i=1,2}$. The set of variational parameters is then given by $\{z_1, z_2, \alpha_1, \alpha_2\}$.

Replacing (7) into the Euclidean action in Eq. (1), we derive the Lagrangian

$$\begin{aligned} L = \sum_j \left\{ -\hbar N_j z_j \dot{\alpha}_j - \frac{\hbar^2 N_j}{2m} \alpha_j^2 - \frac{\hbar^2 N_j}{2m} \left(\frac{1}{\sigma_r^2} + \frac{1}{2\sigma_z^2} \right) \right. \\ \left. - \frac{N_j}{4} m \omega_0^2 (2\sigma_r^2 + \lambda_z^2 \sigma_z^2 + 2\lambda_z^2 z_j^2) - \frac{1}{2} \frac{g_{jj} N_j^2}{2\sqrt{2}\pi^{3/2} \sigma_r^2 \sigma_z} \right\} \\ - \frac{g_{12} N_1 N_2 \exp\left[-\frac{(z_j-z_k)^2}{2\sigma_z^2}\right]}{2\sqrt{2}\pi^{3/2} \sigma_r^2 \sigma_z} + (\text{BMF}). \end{aligned} \quad (8)$$

where the quantum fluctuations contribution in Eq. (3) is simplified by assuming $g_{12}^2 = g_{11}g_{22}$, meaning that we are dealing with the system close to the mean-field instability threshold [50]. The beyond mean field term in the action then reads

$$(\text{BMF}) = \left(\frac{m}{\hbar^2}\right)^{3/2} \int d^3\mathbf{r} (g_{11}|\psi_1|^2 + g_{22}|\psi_2|^2)^{5/2}. \quad (9)$$

In addition, to keep the calculation as analytical as

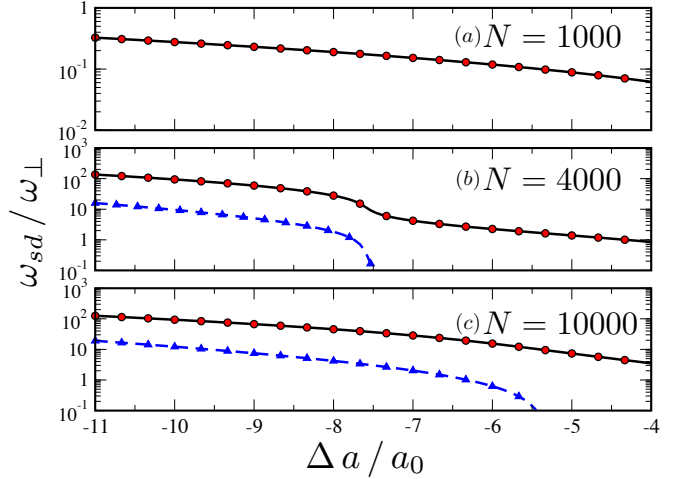


FIG. 4. *Spin dipole oscillations frequencies.* (Red dots) Spin dipole oscillations frequency and (Blue triangles) single-particle emission threshold $-\mu$ for $N = 1000, 4000, 10000$ particles. For $N = 1000$ the chemical potential is positive in the range shown in the figure (soliton regime). In all cases the spin-dipole frequency is higher than $-\mu$ by more than one order of magnitude. The plots shown are done with equal intra-species interaction $g_{11} = g_{22}$.

possible, we consider a symmetric mixture, by taking $g_{11} = g_{22}$ with corresponding equilibrium numbers $N_1 = N_2$. Given the vector of variational parameters \mathbf{q} , the Euler-Lagrange equations are computed from Eq. (8) via $\frac{d}{dt} \frac{\partial L}{\partial \dot{q}_i} - \frac{\partial L}{\partial q_i} = 0$. Accordingly, the equation for the slope $\alpha_i = m \dot{z}_i / \hbar$ is elementary, so its dynamics it is completely determined by the one of z_i . A closed system of (linearized) differential equation can thus be derived straightforwardly

$$\begin{aligned} \ddot{z}_1 + \omega_0^2 \lambda_z^2 z_1 &= \sqrt{\frac{2}{\pi}} \left(\frac{a_{12} \hbar^2 N_1}{m^2 \sigma_r^2 \sigma_z^3} \right) (z_1 - z_2) \\ &\quad - \frac{1024}{25\pi^{1/4}} \left(\frac{a_{11}^{5/2} \hbar^2 N_1^{3/2}}{m^2 \sigma_r^3 \sigma_z^{7/2}} \right) (z_1 - z_2) \quad (10) \\ &\quad (z_1 \rightleftharpoons z_2). \end{aligned}$$

The equation for z_2 has the same structure except for a global sign on the right side of the equation above. The sum of these two equations leads to the equation for the longitudinal motion of the center of mass oscillating with the trap frequency $\omega_0 \lambda_z$ (Kohn's theorem).

Concerning the relative coordinate $\tilde{z} = z_1 - z_2$, we get

$$\ddot{\tilde{z}} + \omega_{\text{rel}}^2 \tilde{z} = 0. \quad (11)$$

By rescaling the length in units of a_{\perp} , the energies in units of $\hbar\omega_{\perp}$, the frequency ω_{rel} of the spin-dipole oscil-

lations reads (in unit of ω_{\perp}^{-1}),

$$\frac{\omega_{rel}^2}{\omega_{\perp}^2} = \lambda_z^2 - \sqrt{\frac{8}{\pi}} \frac{N_1(a_{12}/a_{\perp})}{\sigma_r^2 \sigma_z^3} + \frac{2048}{25\pi^{1/4}} \frac{(a_{11}/a_{\perp})^{5/2} N_1^{3/2}}{\sigma_r^2 \sigma_z^{7/2}}, \quad (12)$$

which, in absence of longitudinal confinement (i.e. $\lambda_z = 0$) is always a positive defined quantity when the effective mean-field interaction is attractive ($\Delta a \lesssim 0$). The results of the numerical analysis of the spin dipole frequencies are summarized in Fig. 4 for a wide range of interactions and different particle numbers. We observe that only in the soliton regime do spin oscillations become observable ($N = 1000$). In the droplet phase self-evaporation is the dominant mechanism.

Concerning Eq. (12), we highlight the different sources of the two terms contributing to spin-dipole oscillations. The first one represents the mean-field attraction between the two-component and thus depends only on a_{12} . Since we are considering the mutual dynamics between the components, it is reasonable that purely intra-component terms do not contribute to ω_{rel} . One has however to consider that Gaussian fluctuations are encoded in Eq. (9) in such a way that it is not possible to split it in two terms, each one referring to one component.

Eq. (12) provides another peculiar feature of self-bound states in binary Bose mixtures: the occurrence of spin-dipole oscillations is not inhibited by turning off the longitudinal confinement, i.e. $\lambda_z = 0$. Indeed, the interplay between the mean-field inter-component attraction and the repulsion arising from quantum fluctuations establishes a restoring force. Then, differently from the mean-field scenario depicted in [44], the presence of a longitudinal confinement is not essential for spin-dipole oscillations to take place due to the attractive nature of the mean-field interaction between the two species.

V. EXPERIMENTAL NUMBERS

By now, experiments on self-bound states of binary Bose mixtures were performed by considering a mixture of ^{39}K atoms in two different internal states, $|1\rangle = |F = 1, m_F = -1\rangle$ and $|2\rangle = |F = 1, m_F = 0\rangle$. By tuning an external magnetic field, Feshbach resonances provide the possibility of exploring a wide range of intra and inter-particles scattering lengths. More precisely [53], by tuning the magnetic field between $B = 54 \div 57.5$ G, where $a_{11} = 33.5 a_0$ and $a_{12} = -53.6 a_0$, the variation of a_{22} provides a whole range of values for Δa , from $-15 a_0$ to $+10 a_0$. Collective oscillations in binary mixtures can be probed in an experimental setup similar to the one developed in [26]. The existence of the soliton-droplet crossover can be revealed by engineering a cigar-shaped mixture and then removing the trapping along the z -axis and observing that the system still has a well-defined longitudinal length.

Our analytical results are compatible with the occurrence of self-evaporation for a large interval of experimental parameters. Only in a small window in the parameters space do we have that where monopole/quadrupole collective oscillations can be in principle observed as highlighted in Fig. 3. Moreover, we developed our analysis in a zero-temperature framework, leaving unanswered the question about what happens for small, but finite temperatures.

In order to test our analytical results concerning the spin dipole oscillations in Eq. (12) and Fig. 3, we require a tighter range of experimental values. In particular, as in [33], we consider the symmetric mean-field ground state given by the condition $a_{11} \simeq a_{22} \simeq 33.5 a_0$ at $B = 54.5$ G, where $a_{12} = -54 a_0$. After a careful tuning of intra- and inter-component scattering lengths, the experimental protocol to probe spin-dipole oscillations is reported in [44]. Indeed, each components in an overlapping initial state can be displaced by applying a magnetic field gradient δB along the longitudinal axis, generated by two coils in anti-Helmoltz configuration. Also, as stated in the previous section, a longitudinal trapping is not mandatory to experimentally probe spin-dipole oscillations, because of the peculiar structure of Gaussian fluctuations contribution to the energy density and the attractive mean-field interaction. Then we emphasize that from the experimental perspective our study may provide insights for the observation of spin dipole oscillations of solitons in a parameter regime which is complementary to that of [44]. Finally, we mention that the effect of three-body losses could be included into a full description of the excitation dynamics. This can done with the inclusion of a term $-i\hbar \frac{L_3}{2} |\psi|^4$ in the right side of the Gross-Pitaevskii equation [54]. A dedicated study will be performed in a future publication.

VI. CONCLUSIONS

In this work we analyzed the behavior of collective modes of two-component BECs with attractive interparticle interactions along the crossover from soliton to self-bound droplets in a quasi one dimensional waveguide. We observed a sharp difference in the collective modes in the two regimes. In the soliton regime modes vary smoothly upon the variation of particle number or interaction strength. On the droplet side collective modes are inhibited by the emission of particles. This mechanism turns out to be dominant for a wide range of particle numbers and interactions. In a small window of particle number range and for intermediate interactions we find that monopole frequency is likely to be observed. In the last part we have studied the spin-dipole modes for the case of equal intraspecies interactions and equal equilibrium particle numbers in the presence of a weak longitudinal confinement. We have found that such modes might be again unobservable as their frequency is higher than the particle emission spectrum by at least one order of

magnitude in the droplet phase. In conclusion, we have found that collective modes provide a complementary way to characterize two-component BECs in an optical waveguide. Moreover they provide a strong signature to distinguish between soliton-like configurations from self-bound droplets. We expect that our work, inspired by experiments in the Barcelona group, may provide a useful indication for further experiments with multi-component BECs.

ACKNOWLEDGEMENTS

T. M. acknowledges CNPq for support through Bolsa de produtividade em Pesquisa n. 311079/2015-6 and the hospitality of Physics Department of the University of Padova and the University of L'Aquila where part of the work was done. L.S. thanks for partial support the 2016 BIRD project *Superfluid properties of Fermi gases in optical potentials* of the University of Padova.

-
- [1] M. R. Matthews, D. S. Hall, D. S. Jin, J. R. Ensher, C. E. Wieman, E. A. Cornell, F. Dalfovo, C. Minniti and S. Stringari, Phys. Rev. Lett. **81**, 243 (1998).
 - [2] D. S. Hall, M. R. Matthews, J. R. Ensher, C. E. Wieman and E. Cornell, Phys. Rev. Lett. **81**, 1539 (1998).
 - [3] D. S. Hall, M. R. Matthews, C. E. Wieman and E. Cornell, Phys. Rev. Lett. **81**, 1543 (1998).
 - [4] I. M. Khalatnikov, Sov. Phys.-JETP **5**, 542 (1957).
 - [5] V. P. Mineev, Sov. Phys.-JETP **40**, 338 (1975).
 - [6] A. F. Andreev and E. P. Bashkin, Sov. Phys.-JETP **42**, 164 (1976).
 - [7] S. Beattie, S. Moulder, R. J. Fletcher and Z. Hadzibabic, Phys. Rev. Lett. **110**, 025301 (2013).
 - [8] M.-S. Chang, Q. Qin, W. Zhang, L. You and M. S. Chapman, Nat. Phys. **1**, 111 (2005).
 - [9] T. Zibold, E. Nicklas, C. Gross and M. K. Oberthaler, Phys. Rev. Lett. **105**, 204101 (2010).
 - [10] G. J. Conduit, A. G. Green and B. D. Simons, Phys. Rev. Lett. **103**, 207201 (2009).
 - [11] L. Salasnich and V. Penna, New J. Phys. **19**, 043018 (2017).
 - [12] S. Liberati, M. Visser and S. Weinfurtner, Class. Quant. Grav. **23**, 3129 (2006).
 - [13] P. E. Larre and N. Pavloff, EPL (Europhysics Letters) **103**, 60001 (2013).
 - [14] S. Butera, P. Öhberg and I. Carusotto, Phys. Rev. A **96**, 013611 (2017).
 - [15] Y. Li, L. P. Pitaevskii and S. Stringari, Phys. Rev. Lett. **108**, 225301 (2012).
 - [16] G. Martone, Y. Li, L. P. Pitaevskii and S. Stringari, Phys. Rev. A **86**, 063621 (2012).
 - [17] Y. Li, G. Martone, L. P. Pitaevskii and S. Stringari, Phys. Rev. Lett. **110**, 235302 (2013).
 - [18] J.-R. Li, J. Lee, W. Huang, S. Burchesky, B. Shteynas, F. C. Top, A. O. Jamison and W. Ketterle, Nature **543**, 91 (2017).
 - [19] D. S. Petrov, Phys. Rev. Lett. **115**, 155302 (2015).
 - [20] D. S. Petrov and G. E. Astrakharchik, Phys. Rev. Lett. **117**, 100401 (2016).
 - [21] H. Kadau, M. Schmitt, M. Wenzel, C. Wink, T. Maier, I. Ferrier-Barbut and T. Pfau, Nature (London) **530**, 194 (2016).
 - [22] I. Ferrier-Barbut, H. Kadau, M. Schmitt, M. Wenzel and T. Pfau, Phys. Rev. Lett. **116**, 215301 (2016).
 - [23] L. Chomaz, S. Baier, D. Petter, M. J. Mark, F. Wächtler, L. Santos and F. Ferlaino, Phys. Rev. X **6**, 041039 (2016).
 - [24] M. Schmitt, M. Wenzel, F. Bottcher, I. Ferrier-Barbut and T. Pfau, Nature (London) **539**, 259 (2016).
 - [25] C. R. Cabrera, L. Tanzi, J. Sanz, B. Naylor, P. Thomas, P. Cheiney and L. Tarruell, Science **359**, 6373 (2018).
 - [26] P. Cheiney, C. R. Cabrera, J. Sanz, B. Naylor, L. Tanzi and L. Tarruell, Phys. Rev. Lett. **120** 135301 (2018).
 - [27] G. Semeghini, G. Ferioli, L. Masi, C. Mazzinghi, L. Wolswijk, F. Minardi, M. Modugno, G. Modugno, M. Inguscio and M. Fattori, arXiv:1710-10890 (2017).
 - [28] F. Wächtler and L. Santos, Phys. Rev. A **93**, 061603 (2016).
 - [29] D. Baillie, R. M. Wilson, R. N. Bisset and P. B. Blakie, Phys. Rev. A **94**, 021602(R) (2016).
 - [30] R. N. Bisset, R. M. Wilson, D. Baillie and P. B. Blakie, Phys. Rev. A **94**, 033619 (2016).
 - [31] A. Macia, J. Sanchez-Baena, J. Boronat and F. Mazzanti, Phys. Rev. Lett. **117**, 205301 (2016).
 - [32] F. Cinti, A. Cappellaro, T. Macrì and L. Salasnich, Phys. Rev. Lett **119**, 215302 (2017).
 - [33] A. Cappellaro, T. Macrì, G. F. Bertacco and L. Salasnich, Scientific Report **7**, 13358 (2017).
 - [34] G. E. Astrakharchik and B. A. Malomed, arXiv:1803.07165 (2018).
 - [35] J. Nespolo, G. E. Astrakharchik, and A. Recati, New Journal of Physics **19**, 125005 (2017).
 - [36] P.G. Kevrekidis, D.J. Frantzeskakis, and R. Carretero-Gonzalez (Eds), Emergent Nonlinear Phenomena in Bose-Einstein Condensates. Theory and experiments (Springer, Berlin, 2007).
 - [37] F. Dalfovo, S. Giorgini, L. P. Pitaevskii and S. Stringari, Rev. Mod. Phys. **71**, 463 (1999).
 - [38] N. Henkel, R. Nath, and T. Pohl Phys. Rev. Lett. **104**, 195302 (2010).
 - [39] T. Macrì, F. Maucher, F. Cinti and T. Pohl, Phys. Rev. A **87**, 061602(R) (2013).
 - [40] F. Cinti, T. Macrì, W. Lechner, G. Pupillo and T. Pohl, Nat. Commun. **5**, 3235 (2014).
 - [41] T. Macrì, S. Saccani and F. Cinti, J. Low Temp. Phys. **177**, 59-71 (2014).
 - [42] F. Wächtler and L. Santos Phys. Rev. A **94**, 043618 (2016).
 - [43] D. Baillie, R.M. Wilson, and P.B. Blakie Phys. Rev. Lett. **119**, 255302 (2017).
 - [44] T. Bienaimé, E. Fava, G. Colzi, C. Mordini, S. Serafini, C. Qu, S. Stringari, G. Lamporesi and G. Ferrari, Phys. Rev. A **94**, 063652 (2016).
 - [45] D. M. Larsen, Ann. Phys. 24, 89-101 (1963).
 - [46] C. D' Errico, M. Zaccanti, M. Fattori, G. Roati, M. Inguscio, G. Modugno and A. Simoni, New J. of Phys. **9**, 223 (2007).

- [47] F. Ancilotto, L. Salasnich and F. Toigo, J. Low Temp. Phys. **171**, 329-340 (2013).
- [48] L. Salasnich, A. Parola and L. Reatto, Phys. Rev. A **66**, 043603 (2002).
- [49] T. Büsch, J. I. Cirac, V. M. Perez-Garcia and P. Zoller, Phys. Rev. A **56**, 2978 (1997).
- [50] L. Pitaevskii and S. Stringari, *Bose-Einstein Condensation* (Oxford University Press, New York, 2003).
- [51] A. Bulgac, Phys. Rev. Lett. **89**, 050402 (2002).
- [52] H.-W. Hammer and D. T. Son, Phys. Rev. Lett. **93**, 250408 (2004).
- [53] C. D'Errico, M. Zaccanti, M. Fattori, G. Roati, M. Inguscio, G. Modugno and A. Simoni, New J. Phys. **9**, 223 (2007).
- [54] M. Wenzel, F. Böttcher, T. Langen, I. Ferrier-Barbut, T. Pfau, Phys. Rev. A **96**, 053630 (2017).